

# Search for Anomalous Single Top Quark Production in Association with a Photon in pp Collisions at $\sqrt{s} = 8$ TeV

Reza Goldouzian for the CMS Collaboration<sup>a</sup>,

<sup>a</sup>*School of Particles and Accelerators, Institute for Research in Fundamental Sciences (IPM)  
P.O. Box 19395-5531, Tehran, Iran*

## Abstract

A search for single top quark production through flavor-changing neutral currents at an anomalous  $tq\gamma$  vertex is performed in proton-proton collisions at a center-of-mass energy of 8 TeV. The analysis is based on a dataset corresponding to an integrated luminosity of  $19.1 \text{ fb}^{-1}$  collected with the CMS detector. The search is performed on events with one isolated photon, one muon and jets in the final state. No evidence for a signal is observed. The upper limits on the branching fractions involving vertices with a top quark, a photon, and an up-quark or charm-quark are determined to be  $BR(t \rightarrow u(c)\gamma) < 0.0161(0.182)\%$ .

**Keywords:** top quark, photon, FCNC

## 1. Introduction

Top quark FCNC interactions are highly suppressed in the Standard Model (SM) by the GIM mechanism (e.g.  $BR(t \rightarrow u\gamma) < 10^{-16}$ ) [1]. In some new physics models, a huge enhancement of top quark FCNC couplings with an up-type quark and a photon is predicted. Such couplings can be parametrized in a model independent effective Lagrangian [2]:

$$\begin{aligned} \mathcal{L}_{eff} = & -eQ_t\bar{u}\frac{i\sigma^{\mu\nu}q_\nu}{\Lambda}(\kappa_{tuy}^L P_L + \kappa_{tuy}^R P_R)tA_\mu \\ & -eQ_t\bar{c}\frac{i\sigma^{\mu\nu}q_\nu}{\Lambda}(\kappa_{tcy}^L P_L + \kappa_{tcy}^R P_R)tA_\mu + h.c. \end{aligned} \quad (1)$$

Where  $\kappa_{tuy}^{L,R}$  and  $\kappa_{tcy}^{L,R}$  represent the strength of  $tuy$  and  $tcy$  anomalous couplings for a left or right handed chirality. The scale  $\Lambda$  is an effective cut-off which conventionally is set to be 172.5 GeV, equal to the top quark mass.

In this report, we review a search for the FCNC-induced anomalous couplings of the type  $tuy$  and  $tcy$  performed with  $\text{fb}^{-1}$  of data collected from 8 TeV pp collisions with the CMS detector [3].

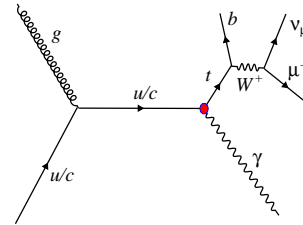


Figure 1: Leading order Feynman diagram for single top quark production via flavor-changing neutral current at the LHC.

## 2. Signal and background modelling

The existence of the anomalous  $tq\gamma$  interactions can lead to the production of a single top quark in association with a photon. One of the representative tree level Feynman diagrams is shown in figure 1. Considering muonic decays of the W boson from top quark decays, the presence of a b-jet, a muon and missing transverse energy (MET) and high  $P_T$  photon characterize the signal signatures.

Separate signal samples for  $tuy$  and  $tcy$  are generated with the PROTOS event generator [4].

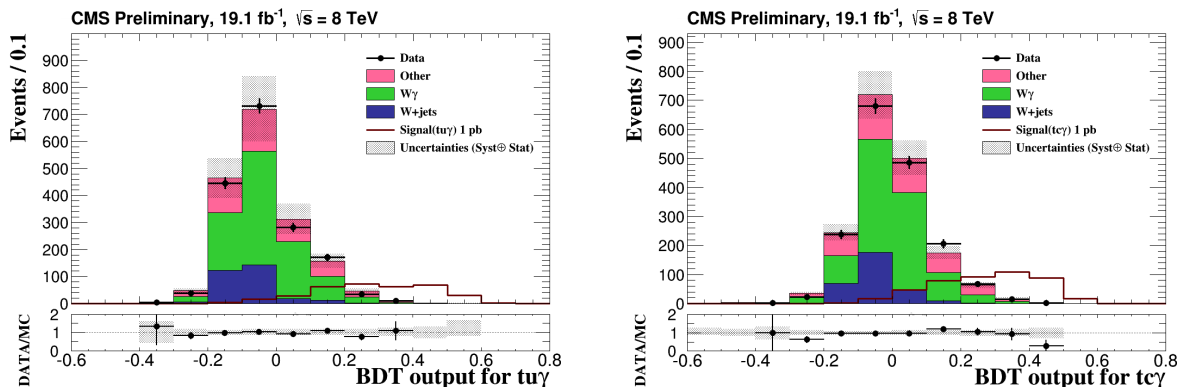


Figure 2: The BDT output distribution for data, all backgrounds, and  $t\gamma u$  (left) and  $t\gamma c$  (right). The  $W+\gamma+jets$  and  $W+jets$  contributions are estimated from data. The  $t\gamma u$  and  $t\gamma c$  signal samples are normalized to a cross section of 1 pb. The uncertainty band include both the statistical and systematic uncertainties.

SM backgrounds are categorized with respect to the detected photon in the final state, into those which have a real prompt photon in final states which are  $W\gamma+jets$ ,  $Z\gamma+jets$ , single top +  $\gamma$ ,  $t\bar{t}\gamma$ ,  $WW\gamma$ ,  $\gamma+jets$  and those in which a jet is misidentified as a photon including Single top,  $t\bar{t}$ ,  $WW$ ,  $WZ$ ,  $ZZ$ ,  $W+jets$ ,  $Z+jets$ .

### 3. Object identification and event selection

Events are preselected by the CMS high level trigger requiring at least one muon with  $P_T > 24$  GeV and  $|\eta| < 2.1$ . The particle-flow algorithm is used for the reconstruction of the all particle candidates [5]. This analysis relies on the reconstruction of photon, electrons, muons, jets and missing transverse energy. Photon candidates are reconstructed as Super-clusters in the electromagnetic calorimeter (ECAL). The inner tracker information is combined with clusters in the ECAL and tracks from the outer muon detector to reconstruct electrons and muons, respectively. The anti- $K_T$  algorithm is used for the jet reconstruction [6]. In order to identify jets originating from b quarks, combined secondary vertex (CSV) algorithm is used [7].

Events are selected if they contain exactly one well isolated photon with  $P_T > 50$  GeV and  $|\eta| < 2.5$  ( $1.442 < |\eta| < 1.566$  is excluded) and contain exactly one isolated muon with  $P_T > 26$  GeV and  $|\eta| < 2.1$ . Events with an additional muon or electron with loose isolation criteria are vetoed. In order to reduce contribution of  $t\bar{t}$ , events with two or more b-jets are rejected. Missing transverse energy is required to be more than 30 GeV.  $\Delta R(l, \gamma)$  and  $\Delta R(b-jet, \gamma)$  are required to be greater than 0.7 to decrease the contribution of radiated photons from high  $P_T$  muon or quarks. Finally, a window is defined around the reconstructed top mass (130

GeV  $< m_{top} < 220$  GeV) to increase the signal to background ratio.

### 4. Background estimation and signal extraction

The contributions of events with a non-prompt photon are not well described by the simulation. A data-driven method is used to estimate the contribution from  $W+jets$  which forms the main background as jets can be misidentified as photons. A control region is defined by reversing the cut on the shower width of the super-cluster and requiring zero b-jets. These requirements lead to a pure region enriched with  $W+jets$  events called  $W+jets$  control region. The contribution from signal events is negligible and the contamination of other SM backgrounds is treated as a systematic uncertainty. Data events in the  $W+jets$  control region are used as  $W+jets$  events in all parts of the analysis. In addition to the shape of the  $W+jets$  background, we need to estimate its normalization in our signal region. The distribution of the  $\cos(W, \gamma)$  variable behaves differently for  $W+jets$ ,  $W\gamma+jets$  and the sum of other SM backgrounds. A template fit is done to the  $\cos(W, \gamma)$  distribution to determine the normalization of  $W+jets$ ,  $W\gamma+jets$  simultaneously.

A multivariate classification approach is chosen to achieve a powerful discriminant between signal events and SM backgrounds. A boosted decision tree (BDT) is constructed and trained using  $tq\gamma$  events for modelling the signal and the sum of  $W\gamma+jets$ ,  $t\bar{t}$  and diboson events for the modelling of the background. The chosen group of variables exploits photon, b-jet and muon transverse momentum,  $\Delta R(\mu, \gamma)$ ,  $\Delta R(b-jet, \gamma)$ , CSV discriminant value for the b-tagged jet, jet multiplicity and  $\cos(top, \gamma)$ .

The BDT output shape of  $W\gamma + jets$  which is an important irreducible SM background in this analysis is estimated from data. The contribution of other backgrounds except  $W\gamma + jets$  is subtracted from data outside of the top mass window to find the BDT output shape of  $W\gamma + jets$  in the signal region.

## 5. Results

The final BDT output for the  $t\bar{u}\gamma$  and  $t\bar{c}\gamma$  signal is shown in figure 2. The signal BDT output distribution is well separated from the background distribution and the data points are well described by the SM prediction. There is no clear evidence for the signal. 95% confidence level (C.L.) upper limits are set on the signal cross section using binned maximum likelihood fit to the BDT output distributions.

The upper limit is affected by several sources of systematic uncertainties which can change either the signal and background yields, or the shape of their BDT discriminator distributions, or both. The systematic uncertainties with instrumental (jet energy scale and resolution, lepton and photon isolation and identification, b-tagging efficiencies and pile-up), theoretical (renormalisation and factorisation scales and PDFs) and data driven background modelling sources are considered in this analysis. In the limit-setting process, the systematic uncertainties are treated as nuisance parameters.

The next-to-leading order QCD corrections of the signal can enhance the signal cross section [8]. The results are summarized in table 1. The obtained limits on the signal cross sections are translated into upper bounds on FCNC anomalous couplings and related top quark branching ratios.

Figure 3 shows the theoretical curve and the 95% C.L. upper limits in the  $(\kappa_{t\bar{u}\gamma}, Br(t \rightarrow \gamma u))$  plane obtained by this analysis. The filled areas correspond to the excluded region. The upper limits obtained by the DELPHI, ZEUS, H1 and CDF collaborations are also shown in the figure for comparison [3, 9, 10, 11, 12].

## 6. Conclusions

A search for anomalous  $t\bar{u}\gamma$  and  $t\bar{c}\gamma$  FCNC interaction through the production of a single top quark and a photon in pp collision data at  $\sqrt{s} = 8$  TeV has been presented. No deviation from the SM prediction is observed and upper limits are placed on the anomalous couplings. The obtained upper bounds are the most stringent limits to date.

Table 1: The observed and expected 95% exclusion limits on the signal cross section, anomalous couplings, and branching ratios with and without including the QCD higher order corrections on the signal cross section.

	Exp. limit (LO)	Obs. limit (LO)
$\sigma_{t\bar{u}\gamma} \times Br(W \rightarrow l\nu_l)$	0.0404 pb	0.0234 pb
$\sigma_{t\bar{c}\gamma} \times Br(W \rightarrow l\nu_l)$	0.0411 pb	0.0281 pb
$\kappa_{t\bar{u}\gamma}$	0.0367	0.0279
$\kappa_{t\bar{c}\gamma}$	0.113	0.094
$Br(t \rightarrow u\gamma)$	0.0279%	0.0161%
$Br(t \rightarrow c\gamma)$	0.261%	0.182%
	Exp. limit (NLO)	Obs. limit (NLO)
$\sigma_{t\bar{u}\gamma} \times Br(W \rightarrow l\nu_l)$	0.0408 pb	0.0217 pb
$\sigma_{t\bar{c}\gamma} \times Br(W \rightarrow l\nu_l)$	0.0410 pb	0.0279 pb
$\kappa_{t\bar{u}\gamma}$	0.0315	0.0229
$\kappa_{t\bar{c}\gamma}$	0.0790	0.0652
$Br(t \rightarrow u\gamma)$	0.0205%	0.0108%
$Br(t \rightarrow c\gamma)$	0.193%	0.132%

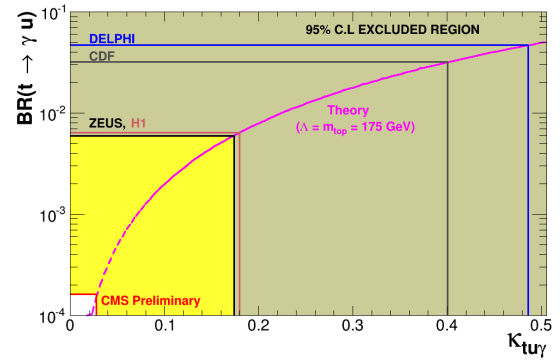


Figure 3: The observed 95% CL upper limit on the  $Br(t \rightarrow \gamma u)$  versus the strength of the anomalous coupling  $\kappa_{t\bar{u}\gamma}$  for the LEP, ZEUS, H1, CDF and CMS collaborations [3, 9, 10, 11, 12].

## References

- [1] S. L. Glashow, J. Iliopoulos and L. Maiani, Phys. Rev. D **2**, 1285 (1970).
- [2] J. A. Aguilar-Saavedra, Acta Phys. Polon. B **35**, 2695 (2004) [hep-ph/0409342].
- [3] CMS Collaboration, CMS-PAS-TOP-14-003.
- [4] J. A. Aguilar-Saavedra, Nucl. Phys. B **837**, 122 (2010) [arXiv:1003.3173 [hep-ph]].
- [5] F. Beaudette [CMS Collaboration], arXiv:1401.8155 [hep-ex].
- [6] M. Cacciari, G. P. Salam and G. Soyez, JHEP **0804**, 063 (2008) [arXiv:0802.1189 [hep-ph]].
- [7] CMS Collaboration [CMS Collaboration], CMS-PAS-BTV-11-004.
- [8] Y. Zhang, B. H. Li, C. S. Li, J. Gao and H. X. Zhu, Phys. Rev. D **83**, 094003 (2011) [arXiv:1101.5346 [hep-ph]].
- [9] CDF Collaboration, Phys. Rev. Lett. **80**, 2525 (1998).
- [10] ZEUS Collaboration, Phys. Lett. B **559**, 153 (2003) [hep-ex/0302010].
- [11] DELPHI Collaboration, Phys. Lett. B **590**, 21 (2004) [hep-ex/0404014].
- [12] H1 Collaboration, Phys. Lett. B **678**, 450 (2009) [arXiv:0904.3876 [hep-ex]].